NASA Technical Memorandum 87108

Refrigerated Dynamic Seal to 6.9 MPa (1000 psi)

Robert C. Hendricks
Lewis Research Center
Cleveland, Ohio

and

R.L. Mullen
Case Western Reserve University
Cleveland, Ohio

and

M.J. Braun
University of Akron
Akron, Ohio

Prepared for the
Cryogenic Engineering Conference and International
Cryogenic Materials Conference
cosponsored by the CEC/ICMC and NBS
Cambridge, Massachusetts, August 12–16, 1985

NASA

REFRIGERATED DYNAMIC SEAL TO 6.9 MPa (1000 psi)

Robert C. Hendricks
National Aeronautics and Space Administration
Lewis Research Center
Cleveland, Ohio 44135

R.L. Mullen
Case Western Reserve University
Dept. of Civil Engineering
Cleveland, Ohio 44106

M.J. Braun
University of Akron
Dept. of Mechanical Engineering
Akron, Ohio 44325

E-2708

SUMMARY

In a refrigerated seal the fluid to be sealed flows through a refrigerated housing or constriction. The fluid can be frozen to the housing during the transient phase. Under steady-state conditions the refrigerated seal proved to be a dynamic low-leakage seal. The concept was extended to pressure differences of 6.9 MPa (1000 psi).

INTRODUCTION

One purpose of a seal is to prevent fluid loss (i.e., to minimize leakage). However, in many instances improperly designed seals have caused failures and deratings of turbomachines. Thus a second and equally important purpose of a seal is the prevention of dynamic instabilities (ref. 1).

In many turbomachine applications, fluids with significantly different boiling points may exist in close proximity. Such fluids could provide the heat sink for a refrigerated seal as discussed in Hendricks (ref. 2*). Flow losses and dynamic parameters such as stiffness and damping can be actively controlled by either the formation of a solid or an increase in the viscosity of the fluid within the narrow aperture. The rotating member must generate energy through viscous dissipation to balance the refrigeration load.

In this study the self-sealing, high-shear flow passage approach of Hendricks (ref. 2) was extended to large pressure differences.

---

*In a note, "Guidelines for Success in Freeze Plugging Pipe," C.L. Schelling, Freeze Seal, Inc., New Castle, Delaware, describes a freezing method to repair valves in lines to 48 in. in diameter by freezing a plug in the line (Ref. Nuclear Safety, 1985).

APPARATUS AND PROCEDURE

An apparatus (fig. 1) was constructed to determine the effectiveness of a self-sealing system at large pressure differences. The fluid to be sealed was water and the refrigerant was nitrogen. Apertures of the small- and large-length-to-diameter-ratio (L/D) Borda types (ref. 3) were used as shaft seals and placed between bearing supports (fig. 2). With the shaft rotating, water was added to the reservoir, which leaked profusely. As the nitrogen cooled an annular region around each seal, the leakage stopped entirely as was also demonstrated in Hendricks (ref. 2) for an orifice and a Borda aperture. Less time was generally required to stabilize the rotor and to seal the system for the large-L/D Borda seals, as would be expected from their better heat transfer and larger contact area. For eccentric seals or those rubbed, misaligned, or badly damaged, the solid plug (ice layer) built up quickly, and with sufficient refrigeration the leak stopped completely.

Once the plug is formed and maintained, the seal should not "wear" and should adjust to system perturbations unless the pressure difference becomes sufficient to fracture the plug. To illustrate this, the water reservoir was filled to capacity, taking care to eliminate all trapped air, and valved off. Using gaseous nitrogen as the pressurant, the water reservoir pressure was increased in 0.3-MPa (50-psi) increments and valved off. If no pressure drop or leaks were observed, the pressure was incremented. At 6.9 MPa (1000 psig) one section of the plug began to leak.

ANALYSIS

Simplified Model

The analysis for a simplified model is given in the appendix. It is shown that in a transient thermal analysis with freezing the calculated clearance became 0.01 cm (0.004 in) and some leakage could be expected. The shear stress calculated from freeze-plug failure data for the small-L/D aperture, 1.03 MPa (150 psi), was in reasonable agreement with the ultimate stress as estimated from the behavior of concrete.

Finite Element Model

Although it was the small-L/D Borda aperture plug that failed, both long and short apertures were modeled (fig. 1). The finite element model (FEM) consisted of 882 and 182 elements for the large- and small-L/D apertures, respectively. In both cases, there were 14 elements in the radial direction, 8 in the ice, and 6 in the steel, leaving 63 and 13 axial elements, respectively (fig. 3). Between 0.715 and 0.750 cm (0.28 and 0.295 in) the steel tube was supported (i.e., fixed); the small-L/D tube started at 0.715 cm. The curvature of the cooling coil was not considered.

The axial pressure profile through the seal was assumed to be linear. Thus loading was that of a thin ice shell with a metal tube backing.

The strength of ice was at best elusive (see appendix); however, from previous experience, the material behavior of ice was assumed to be similar to that of concrete. The modified Pauw relation as adopted by ACI** is

$$E_c = 33\ W \quad Wf_c \tag{1}$$

where E_c is the secant modulus of elasticity (psi), W the unit weight (lb/ft^3), and f_c the ultimate strength (psi). The allowable shear stress on a section for an ultimate strength design is

$$2\varphi \quad f_c < V_{cu} < 3.5\ \varphi \quad f_c = 3.5\ \varphi E_c/(33W^{3/2}) \tag{2}$$

For ice, $E_c = 1x10^6$ psi, $\varphi = 0.85$, $W = 56\ lb/ft^3$, and the shear stress range becomes

$$\begin{gathered} 122\ \text{psi} < V_{cu} < 214\ \text{psi} \\ 0.84\ \text{MPa} < V_{cu} < 1.48\ \text{MPa} \end{gathered} \tag{3}$$

RESULTS

Numerical

In both cases (large- and small-L/D plugs) the shear stress diminished rapidly in the axial direction from the high-pressure side to the low-pressure side of the plug seal with concentrations near the point of fixity (fig. 4). The shear stresses near the high-pressure side were 2.76 and 4.28 MPa (400 and 620 psi) for the large- and small-L/D plug seals, respectively. The average shear stresses were approximately 0.69 and 1.38 MPa (100 and 200 psi), respectively. Anticipating the behavior of ice to be similar to that of concrete, the previously estimated shear stresses were 0.84 to 1.48 MPa (122 to 214 psi), indicating the small-L/D plug seal to be overstressed; both plug seals were overstressed near the high-pressure side.

Experimental

At 6.9 MPa (1000 psig) the plug fractured and water leaked out. The fracture was in reasonable agreement with the simplified and finite element analyses. Instrumentation of the passage would have provided more details for modeling.

Applications

The applications and limitations of a refrigerated seal are discussed in Hendricks (ref. 2). Among the applications are precise seal apertures; quick fix methods; solid formation in hypersonic flows; redundant or emergency seals; enhanced stability; and secondary fluid injection. The seals cannot be used as static seals unless auxiliary heat is available and sufficient housing

** American Concrete Institute Publication ACI 318-83.

(shaft) strength is provided to restrain the volumetric expansion of ice formation. It may also be possible to adaptively control stiffness and damping coefficients by controlling refrigerant flow to minimize system vibrations (including the first critical).

SUMMARY OF RESULTS

A proposed sealing concept where the fluid to be sealed flows through a refrigerated housing or constriction has been extended to pressure differences of 6.9 MPa (1000 psi). As the fluid cools, its viscosity increases and it becomes more resist to leakage. In some cases this may be sufficient to establish the desired leakage rates, but in other applications the temperature must be lowered to below the freezing point of the fluid in the aperture in order to build and maintain a sealing plug.

Under steady operating conditions the viscous dissipation provided by the rotating member maintains a thin liquid film between the shaft and the sealing plug. For the water-nitrogen system axial pressure differences to 6.9 MPa (1000 psi) were maintained. The concept provided a dynamic low-leakage Borda seal.

A finite element method was used to determine the strains induced in the sealing plug. The predictions were in reasonable agreement with the experimental data.

Discussions with Cole (ref. 4) clearly indicate the need for a thermomechanical creep analysis.

SYMBOLS

A	area
b	aperture static clearance
c	aperture dynamic clearance
C_p	specific heat
D	hydraulic diameter
E_c	secant modulus of elasticity
f_c	ultimate strength
G	mass flux
H	latent heat
h	heat transfer coefficient
k	thermal conductivity

L ratio of heat transported by refrigerant to that conducted through solid plug, Eq. (8) (also length)

N ratio of heat input from seal to that absorbed by refrigerant, Eq. (7)

Nu Nusselt number, hD/k

Pr Prandtl number, $C_p\eta/k$

R shaft radius

Re Reynolds number, GD/η

S viscous dissipation

T temperature

t thickness

V_{cu} shear stress, ultimate design

W weight per unit volume

ρ density

Θ dimensionless time in terms of convection, conduction, and latent energies at interface, Eq.(6)

θ time

η viscosity

τ stress

Ω angular velocity

Subscripts:

a coolant side

amb ambient

f fusion or solid

i seal fluid side

m melting

max maximum

n normal

s surface

xc cross section

rz surface normal to r, direction parallel to z

0 reference or stagnation

APPENDIX - SIMPLIFIED ANALYSIS

Thermal

Consider a shaft seal where either the working fluid can solidify or a solid plug can be formed through secondary fluid injection (fig. 5). Further, consider a seal configuration such that the clearance-to-radius ratio $c/R = (b - t)/R$ is much less than 1, so that the problem can then be addressed as one-dimensional; refrigeration is provided through a heat exchanger (fig. 6). In terms of this model the viscous dissipation becomes

$$S = \frac{\eta(R\Omega)^2}{b - t} \tag{4}$$

For a fixed rotational speed Ω, S is directly related to the viscosity η, which generally increases as temperature decreases†, and is inversely proportional to the clearance or the amount of solid plug formed in the seal aperture. As an example, for a 25-mm (1 in) shaft turning at 18 000 rpm in water with cold gaseous nitrogen refrigerant:

1. Cooling the aperture water from 38 to 10 °C (100 to 50 °F) nearly doubled the viscosity and increased the axial pressure drop across the aperture

2. Under equilibrium conditions for $b - t$ of 0.01 mm, S became 6 W/cm^2 (19 000 Btu/hr ft^2). Thus for some applications it may only be necessary to control the temperature of the fluid within the aperture to minimize leakage. Once a solid plug is formed, the energy required to maintain the plug can be small.

A model of the energy transport required to reduce the seal aperture fluid temperature and build a solid plug to provide a clearance of $b - t$ is illustrated in figure 7. An analysis for this geometry follows that presented by Rohsenow (ref. 6). The governing parametric relation is

$$\Theta = \ln \frac{N - 1}{N(L + 1) - 1} - \frac{L}{N} \tag{5}$$

---

†Although infinite at the critical point, viscosity has a minimum in the thermodynamic critical region. At low temperatures (near the triple point) viscosity has a maximum for quantum fluids. The temperature effect is usually strong for liquids, exp (a/T), and weak for gases, $T^{2/3}$. Further, for a synthetic oil such as Mobil RL-714 Stock 509, a temperature change from 60 to 20 °C (140 to 68 °F) increases the viscosity by a factor of 4 (Braun (ref. 5)). One now must consider the stability of operating in the critical region with bearings, etc, as η has a minimum.

where Θ is the dimensionless time to freeze the thickness $b - t$ in terms of conduction to, convection from, and latent heat at the solid-fluid interface.

$$\Theta = \frac{h_a^2 (T_0 - T_f)}{\rho H k} \theta \tag{6}$$

where N is the ratio of the heat input from the seal to that absorbed by the refrigeration,

$$N = \frac{h_i (T_0 - T_f)}{h_a (T_f - T_a)} \tag{7}$$

and L is the ratio of the heat transported by the refrigerant to that conducted through the solid

$$L = \frac{h_a (b - t)}{k} \tag{8}$$

Here ρ and k are properties of the solid plug and H is the latent heat of fusion. The heat transfer coefficients h_a and h_i were determined to sufficient accuracy by using the McAdams equation

$$Nu = 0.023 \, Re^{0.8} Pr^{0.4} \tag{9}$$

even though more sophisticated forms are available.

For gaseous nitrogen refrigerant (T = -193 °C (-316 °F), P = 0.138 MPa (20 psia)) flowing at 3 m/s (10 ft/s) through a 4.6-mm (0.18-in) diameter tube, the Reynolds number Re was 12 400 and h_a was 70 W/m^2 K (12 Btu/hr ft^2 °F). On the water side, for a leakage velocity of 1.8 m/s (6 ft/s) with a hydraulic diameter (2c) of 2.5 mm (0.1 in), the Reynolds number became 3500 and h_i was 9000 W/m^2 K (1600 Btu/hr ft^2 °F). For large $T_0 - T_f$ freezing will not occur. However, at $T_0 \rightarrow T_f$, (a reasonable assumption for the Borda inlet) an explicit solution is found

$$\Theta = \frac{(L + 1)^2 - 1}{2} \tag{10}$$

As an example, consider the apparatus of figure 5 (Hendricks (ref. 2)). Using equations (6), (8), and (10) and the properties of ice, with b = 1.2 mm (0.05 in) (i.e., t = 0), an ice plug should form in at least 1/2 min. The actual "pinch off" clearance $b - t$ was self-limiting; for as soon as the clearance became very small, S became large and melted the ice. An additional feature was that the maximum temperature occurred within the aperture channel and not at the rotating shaft, thereby preventing complete closure so long as the shaft was rotating.

Mechanical

The ice plug can be represented as a cylinder of thickness t (clearance), length L (length of Borda), and radius R_0 (shaft radius), fully bonded to the small- or large-L/D Borda inlet (fig. 8). Although the adhesive/

cohesive strength can vary with temperature and surface characteristics, we assumed it to be uniform. One end of the cylinder was loaded at P_0 and the other was at P_{amb}. The axial pressure distribution in the clearance gap was parabolic, but previous work with fluid nitrogen and hydrogen has shown that a linear approximation is satisfactory (Hendricks and Stetz (ref. 7)). As such the average uniform radial load is $(P_0 + P_{amb})/2$.

Under these conditions a concrete-footer-slab model was used to simulate the behavior of the ice plug. Balancing the forces on the model gave

$$\tau A_s = (P_0 - P_{amb}) A_{xc} \tag{11}$$

and the shear at failure became

$$t = \frac{\Delta P t}{L} = 1000 \times \frac{0.03}{0.2} = 1.03 \text{ MPa (150 psi)} \tag{12}$$

The allowable shear based on ultimate strength, which in turn was based on modulus of elasticity, varied between 0.8 and 1.5 MPa (115 and 215 psi), which was in reasonable agreement with equation (12).

Note that the pressure difference restrained by the ice depended on seal length and clearance and on the compressive and adhesive/cohesive strength of the ice. Although we assumed the ice to be fully bonded to the steel, the strength depended on the rate of freezing and the temperature-pressure history as well as on substrate characteristics.

Discussions with Cole (ref. 4) and his work demonstrate that grain size d, creep rate ε, temperature T, applied load σ, and confining pressure all affect the strength and failure of ice (in our case type I_h). For example, at -5 °C (22 °F) the strength peaks near 10 MPa (1450 psi) for ε 10^{-3} s^{-1} and decreases to 1 MPa for ε 10^{-5} s^{-1}. At -196 °C (-320 °F), the strength range is 21 to 48 MPa (3 to 7 ksi) for P near ambient to over 160 MPa (23 ksi) for 50 MPa < P < 150 MPa (7.2 ksi < P < 22 ksi), (Durham et al. (ref. 8)). When these values are applied to the seal, the solid near the water-ice interface would be at high strain and low strength, and the solid near the nitrogen cooling coil would have a much higher strength. Increasing the confining pressure and surface area should significantly increase the capacity of the Borda seal over that of the orifice seal. These discussions clearly indicate the need for a thermomechanical analysis including the effects of the parameters ε, d, T, σ, and P.

REFERENCES

1. "Rotordynamic Instability Problems in High-Performance Turbomachinery," NASA Lewis Research Center, Cleveland (1980). NASA CP-2133. See also NASA CP-2250 (1982) and NASA CP-2338 (1984).

2. R.C. Hendricks, "A Refrigerated Dynamic Seal," NASA Lewis Research Center, Cleveland (1983). NASA TM-83378.

3. R.C. Hendricks and T.T. Stetz, "Flow Through Axially Aligned Sequential Apertures of the Orifice and Borda Types," NASA Lewis Research Center, Cleveland (1981). NASA TM-81681.

4. David M. Cole, CRREL, Box 282, Hannover, NH.

5. M.J. Braun and R.C. Hendricks, "An Experimental Investigation of Vaporous/ Gaseous Cavity Characteristics of an Eccentric Journal Bearing," American Society of Lubrication Engineers, Park Ridge, Illinois (1982).

6. W.M. Rohsenow and J.P. Hartnett, eds., "Handbook of Heat Transfer," McGraw-Hill, New York (1973).

7. R.C. Hendricks and T.T. Stetz, Studies of Flows Through N-Sequential Orifices, J. Fluids Engr. 106:297 (1983).

8. W.B. Durham, H.C. Heard, and S.H. Kirby: Experimental Deformation of Polycrystalline H_2O Ice at High Pressure and Low Temperature: Preliminary Results. J. Geophysical Res. 88 (1983) Supplement pp. B377-B392.

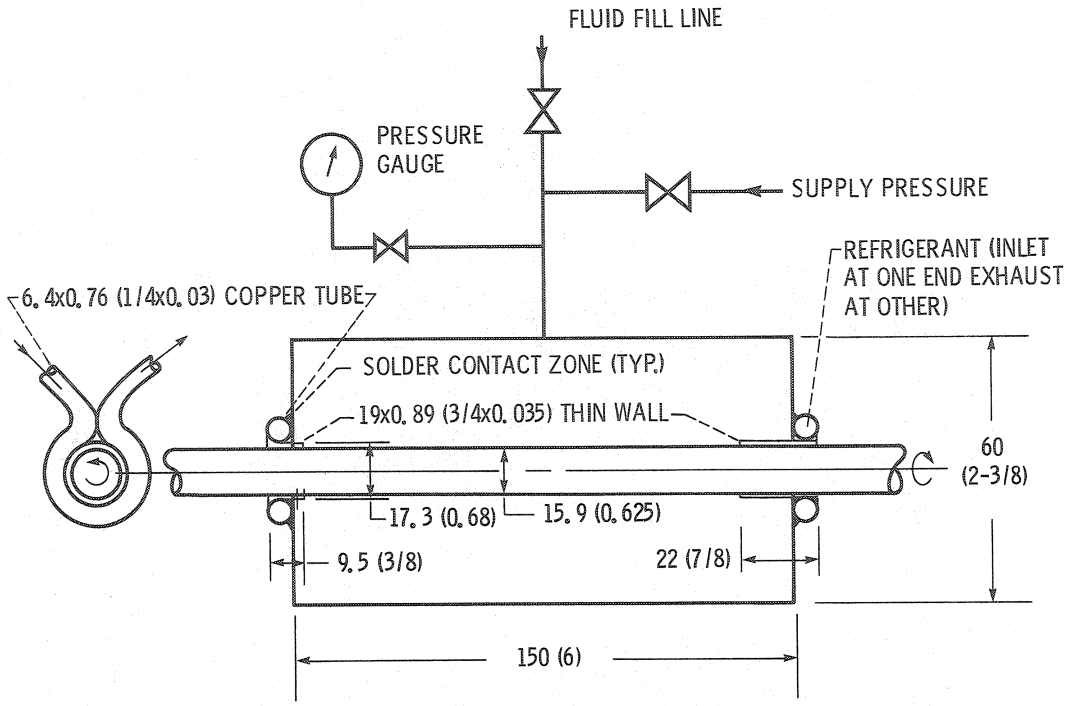

Fig. 1 Schematic of test apparatus for small- and large-Borda type of refrigerated seals. (Dimensions are in millimeters (inches).)

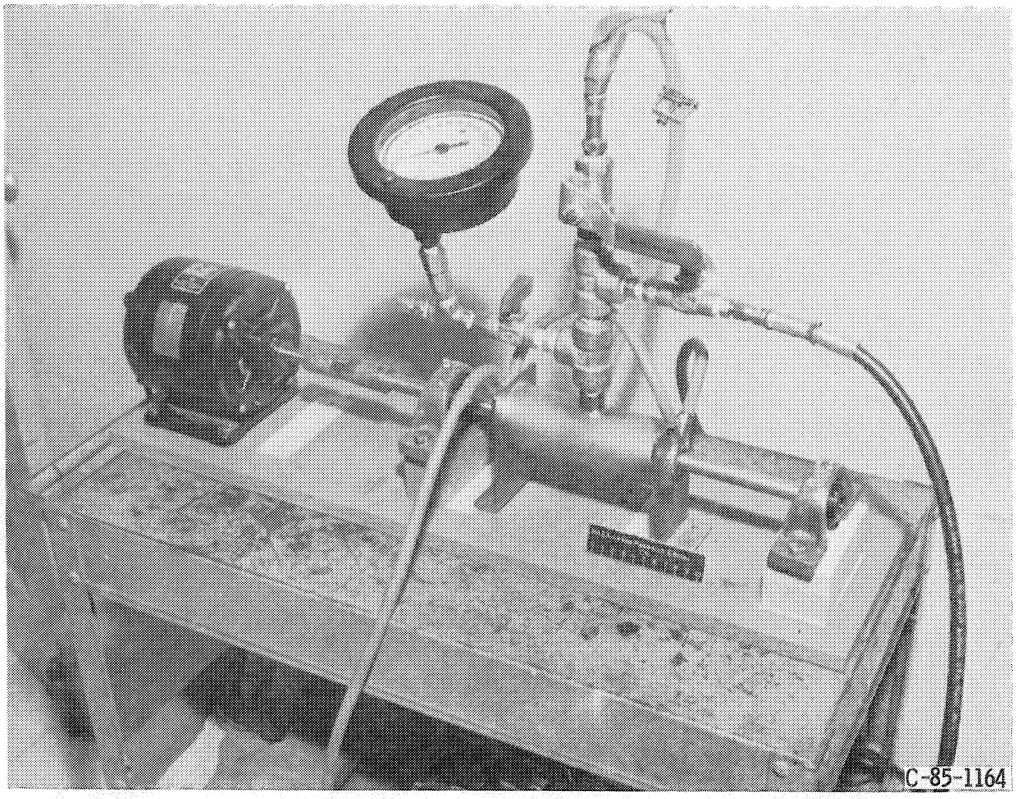

Figure 2. - Refrigerated-seal apparatus.

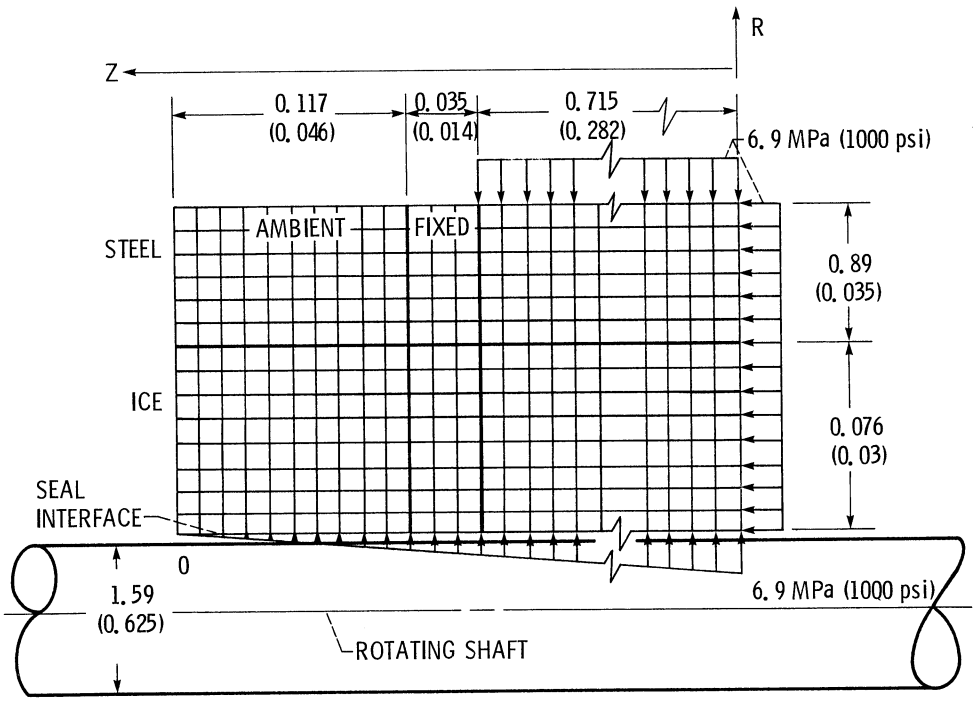

Fig. 3 Finite element model of freeze plug seal. (Dimensions are in centimeters (inches).)

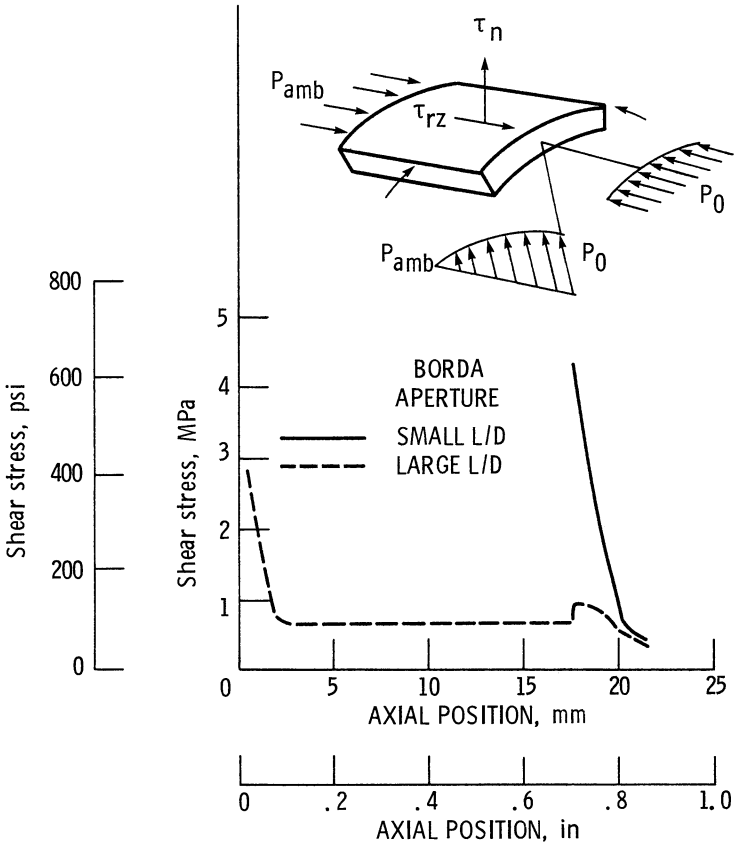

Fig. 4 Shear stress at ice-steel interface.

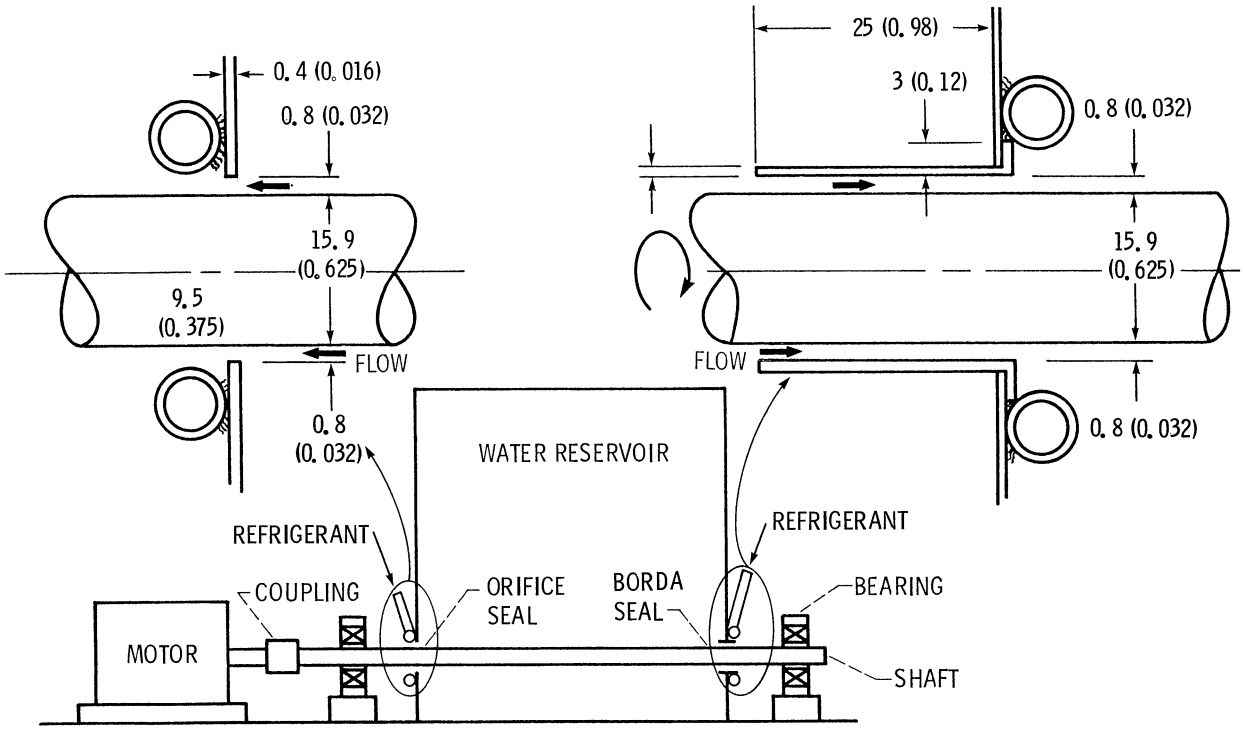

Fig. 5 Schematic of experimental test apparatus for Borda and orifice types of refrigerated seals. (Dimensions are in millimeters (inches).)

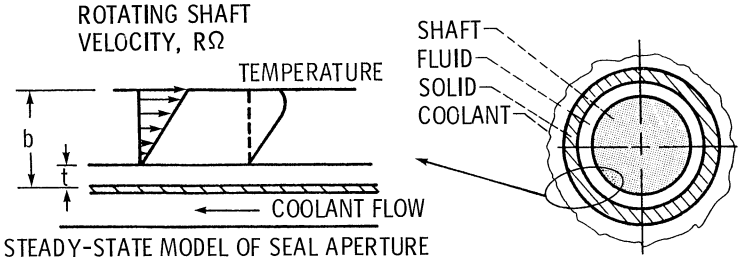

Fig. 6 Schematic of velocity and temperature profiles for refrigerated-seal configuration.

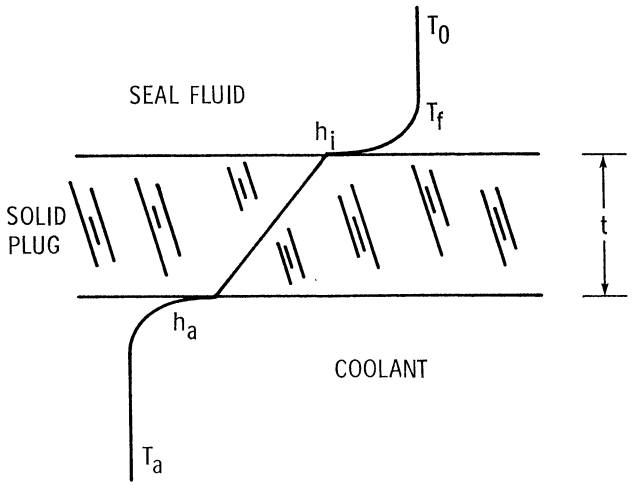

Fig. 7 Temperature profile for refrigerated-seal model.

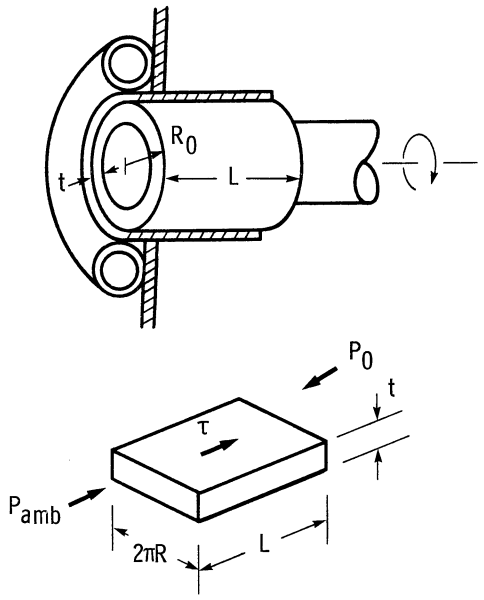

Fig. 8 Slab model simulation of ice plug seal.

1. Report No.	2. Government Accession No.	3. Recipient's Catalog No.
NASA TM-87108		

4. Title and Subtitle	5. Report Date
Refrigerated Dynamic Seal to 6.9 MPa (1000 psi)	
	6. Performing Organization Code: 553-13-00

7. Author(s)	8. Performing Organization Report No.
R.C. Hendricks, R.L. Mullen, and M.J. Braun	E-2708
	10. Work Unit No.

9. Performing Organization Name and Address	11. Contract or Grant No.
National Aeronautics and Space Administration Lewis Research Center Cleveland, Ohio 44135	
	13. Type of Report and Period Covered: Technical Memorandum

12. Sponsoring Agency Name and Address	14. Sponsoring Agency Code
National Aeronautics and Space Administration Washington, D.C. 20546	

15. Supplementary Notes

R.C. Hendricks, NASA Lewis Research Center; R.L. Mullen, Case Western Reserve University, Dept. of Civil Engineering, Cleveland, Ohio 44106; M.J. Braun, The University of Akron, Dept. of Mechanical Engineering, Akron, Ohio 44325. Prepared for the Cryogenic Engineering Conference and Internal Cryogenic Materials Conference cosponsored by the CEC/ICMC and NBS, Cambridge, Massachusetts, August 12-16, 1985.

16. Abstract

In a refrigerated seal the fluid to be sealed flows through a refrigerated housing or constriction. The fluid can be frozen to the housing during the transient phase. Under steady-state conditions the refrigerated seal proved to be a dynamic low-leakage seal. The concept was extended to pressure differences of 6.9 MPa (1000 psi).

17. Key Words (Suggested by Author(s))	18. Distribution Statement
Seals Dynamics Freezing Ice	Unclassified - unlimited STAR Category 34

19. Security Classif. (of this report)	20. Security Classif. (of this page)	21. No. of pages	22. Price*
Unclassified	Unclassified		

*For sale by the National Technical Information Service, Springfield, Virginia 22161